JOURNAL OF CHEMICAL & ENGINEERING DATA

ARTICLE

pubs.acs.org/jced

Site Energy Distribution Function for the Sips Isotherm by the Condensation Approximation Method and Its Application to Characterization of Porous Materials

K. Vasanth Kumar,[*,†] Juan Carlos Serrano-Ruiz,[†] Hiléia K. S. Souza,[‡] Ana María Silvestre-Albero,[†] and Vinod Kumar Gupta[*,§,∥]

[†]Laboratorio de Materiales Avanzados, Departamento de Química Inorgánica, Universidad de Alicante Ctra., San Vicente, s/n-03600 San Vicente del Raspeig, Spain

[‡]REQUIMTE, Departamento de Engenharia Química, Faculdade de Engenharia, Universidade do Porto, Rua Dr. Roberto Frias, 4200-465 Porto, Portugal

[§]Department of Chemistry, Indian Institute of Technology Roorkee, Roorkee 247667, India

[∥]Chemistry Department, King Fahd University of Petroleum and Minerals, Dhahran, Saudi Arabia

ABSTRACT: A site energy distribution function is proposed that can rapidly generate the binding energy distribution of any adsorbent for any target molecules using only the Sips isotherm parameters, the advantages of which are discussed. The proposed model is successfully applied to determine the site energy distribution of a series of activated carbons, activated carbon fiber, and single-wall carbon nanotubes (SWCNT) for the adsorption of several gas molecules. The proposed model revealed the fact that the sorption capacity of the activated carbons for the target molecule depends on the shape and the size of the binding site energies. The proposed model is very simple to use and does not need any complicated or sophisticated computer programs to determine the distribution of binding energies on the adsorbent surface.

INTRODUCTION

Characterization of the site energy distribution of adsorbents for target molecules is needed in many applied problems of adsorption. Characterization of binding site energies can explain how tight the molecules are bound to the surface. Site energy distributions can also be used to estimate the complex problems involved in the competition among solutes for energetically heterogeneous surfaces and also can be used to study the distribution of high- and low-energy binding sites on different activated carbons or other solid surfaces for the target molecules.

The binding energy of any adsorbent for a target molecule can be determined easily from adsorption isotherms, as any theoretical isotherm implicitly reflects the underlying assumptions about the site energy distribution. Theoretically, isotherm parameters can be related to particular site energy distributions, and their empirically determined values can be interpreted with respect to the energetic character of the adsorbent.[1]

A discrete binding (bi-Langmuir) model that assumes a bimodal distribution of binding sites is the most widely used approach for calculating the binding parameters.[2,3] However, the binding parameters determined by this method have limited use as they are sensitive to the number and position of the tangents drawn in the bi-Langmuir model or the so-called Scatchard plot.[2,3] In general, the surfaces of porous adsorbents such as activated carbon, silica gel, alumina, and molecularly imprinted polymers have complex geometrical structures of varying affinity for the guest molecule, and the adsorption phenomenon is related to the characteristic interactions between the adsorbent and adsorbed molecules. Thus, for these types of heterogeneous materials, the Scatchard plot based on a bi-Langmuir isotherm may not provide complete information about the site heterogeneity of the adsorbent, and thus a more realistic model that can explain the actual distribution of site energies is needed for such materials. Previously some researchers who were working in the field of liquid phase adsorption systems proposed some genuine mathematical functions to generate a binding affinity spectrum which is a thermodynamic function of energy based on some theoretical isotherms following several assumptions and approximations.[4,5] In this study, we proposed a mathematical function using Cerofoloini's[6] *condensation approximation method* that can generate the energy spectrum of adsorbent utilizing the Sips isotherm. A site energy distribution function for the Sips isotherm would be very useful as this isotherm was proved to be a successful isotherm to explain the adsorption of several gas molecules. The practical utility and the advantages of the proposed model are discussed based on the application examples of (i) N_2 adsorption at 77 K by a series of activated carbons, (ii) CO_2 adsorption by SWCNTs at 273 K, and (iii) trichloroethylene adsorption onto ACFs at 298.15 K.

EXPERIMENTAL SECTION

A series of activated carbons were prepared by combining chemical and physical activation of olive stones as a precursor. Initially, the lignocellulosic precursor (particle size between (1.7 and 2.0) mm) was impregnated with an aqueous solution of $ZnCl_2$ at 358 K during 7 h under stirring. After the impregnation,

Received: November 18, 2010
Accepted: March 7, 2011
Published: March 23, 2011

dx.doi.org/10.1021/je101240f | *J. Chem. Eng. Data* 2011, 56, 2218–2224

the sample temperature was increased up to 373 K to evaporate part (70 %) of the remaining solution, the final sample being filtered and dried overnight at 353 K. The impregnated sample was submitted to a heat treatment (2 K·min^{-1}) under a flow of N_2 (100 cm^3·min^{-1}) at 773 K for 3 h. After cooling to room temperature, the carbonized sample was washed with diluted HCl acid (10 %) until complete removal of $ZnCl_2$, followed by washing with distilled water until pH 7. Finally, the clean sample was carbonized under a N_2 flow (100 cm^3·min^{-1}) at 1123 K for 2 h. The as-synthesized sample was labeled AC0. In a second step, the sample A0 was submitted to physical activation with CO_2 (100 cm^3·min^{-1}) at 1098 K using different periods of time, i.e., (20, 40, 60, 72, and 80) h, which corresponds to a burnoff of (22, 30, 48, 58, and 70) %, respectively. The samples were labeled AC followed by the activation time used in each case. No discussion has been made about the porous or in general the physicochemical characteristics of these adsorbents, and for this the readers are suggested to refer works of Silvestre-Albero et al.[7]

SITE ENERGY DISTRIBUTION FUNCTION

The three-parameter Sips isotherm that can represent saturation at high pressure and the Freundlich isotherm at low pressures is[8,9]

$$n = \frac{n_{max} K_s P^{m_s}}{1 + K_s P^{m_s}} \quad (1)$$

where n_{max} is the maximum adsorption capacity of the adsorbents for target molecules; K_s is the Sips isotherm constant; and m_s is the Sips isotherm exponent, which should fall within the range from −1 to +1. The Sips isotherm constants, n_{max}, K_s; and m_s can be determined by a simple nonlinear regression analysis. In this study, we performed the nonlinear regression analysis by minimizing the error distribution between experimental data and the Sips isotherm by maximizing the error function, coefficient of determination, r^2, using the Solver add-in, Microsoft (MS) Spreadsheet, MS Excel, MS Corporation.

The site energy distribution of an adsorbent can be determined from the theoretical isotherm from the solution of the adsorption integral (eq 2) to generate the corresponding affinity distribution[5]

$$q_e(p) = \int_{E_{min}}^{E_{max}} q_e(E,p) f(E) dE \quad (2)$$

Equation 2 assumes the total adsorption of gas molecules, q_e, by a heterogeneous surface as the integral of energetically homogeneous isotherm (q_h) multiplied by a site energy frequency distribution, $f(E)$. E_{min} and E_{max} are the limits of energy space that are directly related to the maximum and minimum pressure in the adsorption isotherm. Equation 2, the Fredholm integral equation of the first kind, is difficult to solve and has no general analytical solution. Considering the importance of this expression, several approximate solutions have been developed.[1−3,5] In this study, one of the widely accepted methods of solution usually called the *condensation approximation* method, originally proposed by Cerofolini,[6] was used. In this method, the true kernel is replaced by a condensation isotherm (in this study this refers to the Sips isotherm). Previously, Carter et al.[10] used this method to generate a series of energy distribution functions based on the Langmuir−Freundlich and Freundlich isotherms. In this study we used the Sips (eq 1) isotherm as this isotherm can represent most of the gas phase adsorption systems. According to this method, the equilibrium pressure is related to the energy of adsorption given by[10]

$$p = p_s \exp\left(-\frac{E^*}{RT}\right) = p_s \exp -\left(\frac{E - E_s}{RT}\right) \quad (3)$$

where E is the lowest physically realizable energy and E_s is the sorption energy corresponding to $p = p_s$.[10]

Incorporation of eq 3 into eq 2 will lead to an approximate site energy distribution, $f(E^*)$, which is the differentiation of the isotherm, $q(E^*)$, with respect to E^*

$$f(E^*) = -\frac{dq(E^*)}{dE^*} \quad (4)$$

Equation 4 can be used to determine the site energy distribution function by differentiating the corresponding isotherm expression with respect to E^*. Thus, $f(E^*)$ for the Sips isotherm can be obtained by applying eq 3 for the equilibrium pressure in eq 1 and differentiating the resulting expression with respect to E^*

$$f(E^*) = \frac{\exp\left(-\frac{m_s E^*}{RT}\right) k_s m_s n_{max} p_s^{m_s}}{\left(\exp\left(-\frac{m_s E^*}{RT}\right) k_s p_s^{m_s} + 1\right)^2 RT} \quad (5)$$

Equation 5 is a typical expression that will generate a unimodal or exponential curve depending on the pressure, which are the implicit assumptions or the limiting conditions of the Sips isotherm. The complete derivation of eq 5 appends this article in the Appendix. Since the site energy distribution function defined in eq 5 is directly related to the experimental isotherm, the energy distribution determined by this method is controlled by the range of pressure described in the experimental isotherm.[2] The area under the distribution curve and the spread of the distribution are controlled by the maximum adsorption capacity and the heterogeneity factor, m_s, respectively.

APPLICATION EXAMPLES

The applicability of the proposed model was demonstrated by estimating the energy distribution of a series of activated carbons, A0, A20, A60, A72, and A80, developed in our laboratory[7] for N_2 gas molecules at 77 K. The main objective of this study is only to study the applicability of the Sips isotherm in estimating the site energy distribution of these activated carbons, and no attempts have been made to characterize these adsorbents in detail. The detailed physicochemical characteristics of these adsorbents are explained elsewhere.[7] The experimental equilibrium data were fitted to the Sips isotherm by a nonlinear regression analysis. The nonlinear regression analysis involves a trial and error method which involves the process of minimizing the error distribution between experimental data and the Sips isotherm. The error minimization was done by maximizing the coefficient of determination, r^2, using Solver, add-in, Microsoft Spreadsheet, Microsofot Excel, Microsoft Corporation. Figure 1 shows the experimental data and the fitted Sips isotherm for the adsorption of N_2

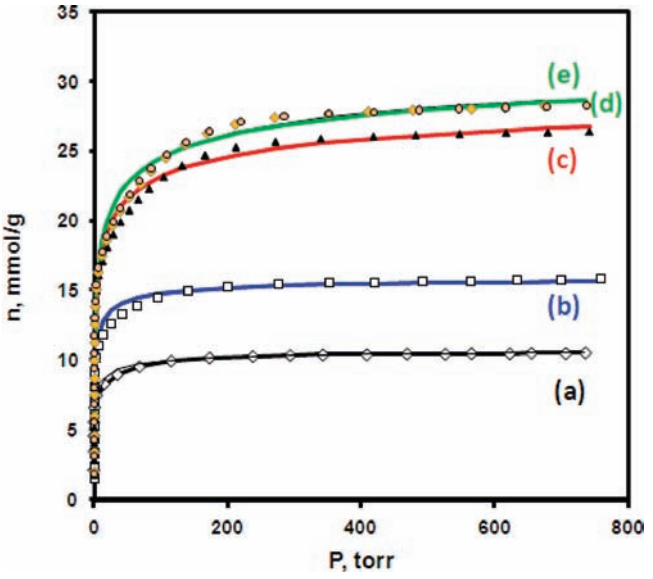

Figure 1. Experimental data and Sips isotherm for the adsorption N_2 onto a series of activated carbons: (a) AC0; (b) AC20; (c) AC60; (d) closed squares, AC72; (e) circles, AC80.

molecules by different activated carbons. The calculated isotherm parameters and the determined r^2 values are given in Table 1. From Figure 1, it can be observed that the experimental data are well represented by the Sips isotherm with higher r^2 values ranging from 0.955 to 0.980. The higher r^2 values and the fitting curves in Figure 1 clearly show that the Sips isotherm can be reasonably used to explain the equilibrium adsorption of nitrogen molecules at 77 K onto these series of activated carbons. Since, as we found that the Sips isotherm well represents the experimental data, it can be safely concluded that the obtained isotherm constants from this equation can reasonably generate the energy distribution spectra of these adsorbents within the studied range of pressure.

To find the binding site energy distribution of these adsorbents, we substituted the determined isotherm parameters (Table 1) of the activated carbons in the site energy distribution function (eq 5) obtained earlier in this study. It is worthwhile to point out that, although eq 5 has no mathematical restrictions, it will predict negative energy values that do not have any physical meaning for the condition of $E < E_s$. Thus, it is important to mention that any site energy distribution curve generated using eq 5 is valid only for the range of pressures in the adsorption isotherm. Figure 2 shows the binding site energy distribution of the activated carbons that are generated using the procedure explained above. From Figure 1, it can be observed that the energy distribution of AC0, AC20, and AC60 exhibits a unimodal distribution of binding sites with two characteristic regions: (i) a unimodal peak corresponding to low-energy binding sites and (ii) an asymptotically decaying region corresponding to high-energy binding sites. In the case of A72 and A80, we observed that the site energy distribution function is exponentially distributed throughout the range of pressure studied. Instantly, these observations indicate to us that these AC72 and AC80 are relatively more heterogeneous than other activated carbons as the site energy distribution is exponential covering the higher binding energy sites. The differences in the binding site energy

Table 1. Sips Isotherm Parameters Determined by Nonlinear Regression Analysis for the Sorption of Nitrogen by a Series of Activated Carbons, Trichloroethylene/Activated Carbon Fiber, and CO_2/Single-Wall Carbon Nanotube Adsorption Systems

adsorption system/experimental condition	isotherm parameters	
trichlorethylene/	n_m	4.36
ACF at 298.15 K	K_s	12.78
	m_s	0.726
	r^2	0.977
CO_2/SWCNT at 273 K	n_m	233.24
	K_s	0.10
	m_s	0.77
	r^2	0.999
N_2/AC0 at 77 K	n_m	11.021
	K_s	1.12
	m_s	0.45
	r^2	11.02
N_2/AC20 at 77 K	n_m	16.25
	K_s	1.09
	m_s	0.487
	r^2	0.955
N_2/AC60 at 77 K	n_m	19.32
	K_s	0.923
	m_s	0.457
	r^2	0.969
N_2/AC70 at 77 K	n_m	31.54
	K_s	0.553
	m_s	0.350
	r^2	0.977
N_2/AC80 at 77 K	n_m	34.30
	K_s	0.469
	m_s	0.365
	r^2	0.975

distribution and the frequencies confirm the structural differences in these adsorbents. The structural differences in these carbons are expected, as we observed earlier that the physical activation of AC0 altered the porous structure of this carbon as confirmed by the increase in the micropore volume. From here on, we refer to AC0 as the reference carbon for the sake of convenience. Our earlier studies[9] showed that these increases in micropore volume are attributed to the process of new pore openings and to the deepening of the existing ones. Figure 2 shows that the binding site energy of the reference activated carbon AC0 and the carbons that correspond to AC0 with (22 and 48) % burnoff (i.e., AC20 and A60) are unimodally distributed for the range of pressures in the experimental adsorption isotherm. Figure 2 also shows that binding site energy also increased the width and the peak of the unimodal distribution curve. This shows that physical activation of the sample AC0 alters both the structure and the breadth of the heterogeneity for the adsorption of N_2 molecules. The exponential distribution of the binding sites in the case of A72 and A80 indicates that the activation conditions with a burnoff percentage of 58 % and 70 % greatly altered the binding site properties making a shift from unimodal to exponential distribution of the binding sites. In other words, we could say that the physical activation of the reference sample corresponding to a burnoff

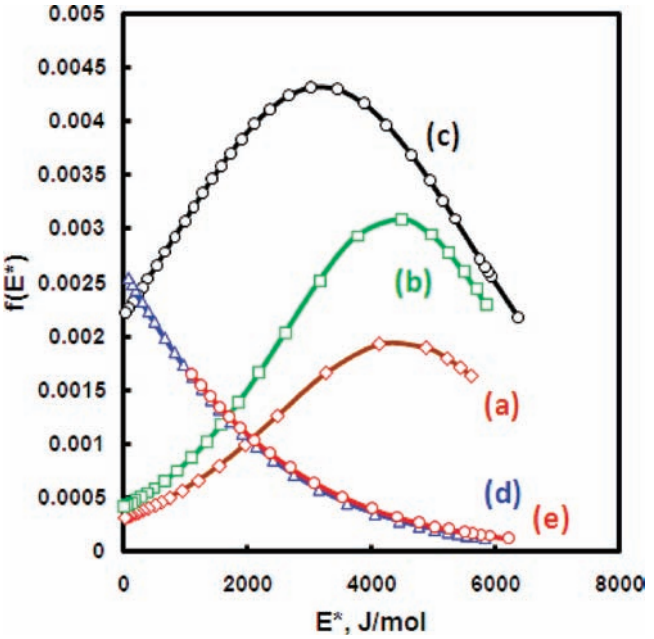

Figure 2. Site energy distribution of activated carbon series A0−A80 for the adosrption of N_2 at 77 K: (a) AC0; (b) AC20; (c) AC60; (d) AC72; (e) AC80.

condition of 58 % (AC72) and 70 % (AC80) created binding sites that preferentially sample gas molecules with higher energies, and they also increase exponentially with an increase in pressure through the entire range of pressures, P_{min} to P_s, where P_{min} here refers to the minimum pressure recorded during the experiments. In addition, we found that the binding site energy distributions are nearly the same for both of these samples with AC80 being slightly more heterogeneous than AC72. This shows that both of these activated carbons could be structurally similar, and the total number of gas molecules that can be sampled on these adsorbents may be similar. This is in good agreement with our earlier findings that both of these carbons have nearly the same pore volume which is in good agreement with similar adsorption. Another interesting observation that can be found from Figure 2 is that the activated carbons whose binding sites are exponentially distributed have the highest uptake capacity for the nitrogen molecules at 77 K. On the basis of this observation, it can be roughly concluded that the more the heterogeneity, the more likely is the probability of the nitrogen molecules being over the adsorption sites. Though this conclusion is an exaggeration based on the results observed for the series of activated carbons in this study, it still can be verified with other systems, which is beyond the scope of this study.

To see the global usefulness of the $f(E^*)$ obtained in this study, the proposed model was further applied to estimate the binding site energy distribution of two more adsorption systems reported in the literature:[11,12] (i) trichloroethylene onto activated carbon fiber and (ii) CO_2 onto single-wall carbon nanotubes. Figure 3 shows the site energy distribution of activated carbon fiber and SWCNT according to eq 5 for the adsorption of tricholorethylene and CO_2, respectively. From Figure 3, it can be observed that the energy distribution of SWCNT exhibits a unimodal distribution of binding sites with a unimodal peak corresponding to low-energy binding sites and an

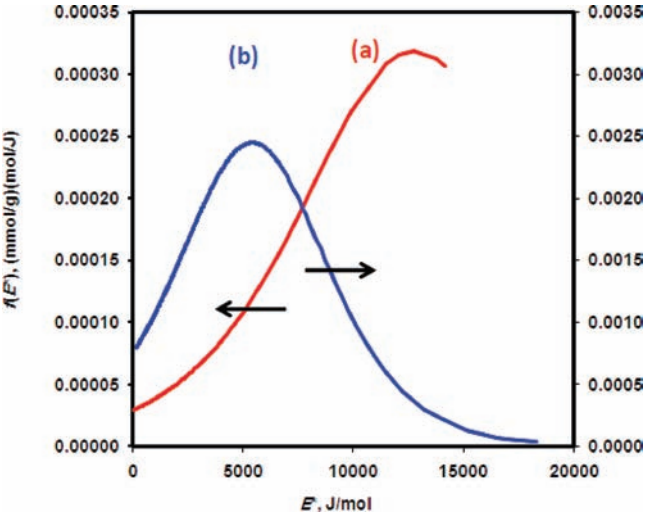

Figure 3. Site energy distribution of trichloroethylene/activated carbon fiber (a) and single-wall carbon nanotube (SWCNT) (b) determined by Sips isotherm for different target molecules.

asymptotically decaying region corresponding to high-energy binding sites. In the case of activated carbon fiber, it can be observed from Figure 3 that the site energy distribution function does not predict or cover the distribution of binding sites with relatively higher energies. This could be expected due to the poor fitting of the experimental data in the relatively low-pressure regime of the isotherm at the studied experimental conditions. However, an extrapolation of the energy distribution curve (not shown) globally indicates that the energies of the binding sites are unimodally distributed.

The site energy distribution of the studied adsorbent materials which differ by physicochemical characteristics clearly indicates that the Sips isotherm can be very useful in estimating the binding site energy distribution of the porous materials. In this study, our aim is only to present a useful expression that allows calculation of or comparison of the performance of any adsorbent using only the Sips isotherm parameters. The Sips isotherm can serve as an alternate to the methods available for determining the heterogeneity from isosteric heat or from thermodynamic parameters.[13−20] The site energy distribution will also give information about how tight the molecules bind to the adsorbent surface in addition to the number of binding sites. Further, the intensity and the spread of the site energy distribution determined using the proposed function can help to identify the difference in structure and the complexity of the heterogeneity of the adsorbent materials.

CONCLUSIONS

The energy distribution function proposed in this study was found to be a useful expression for predicting the site energy distribution of heterogeneous surfaces using only the Sips isotherm parameters. An energy distribution function based on the Sips isotherm suggested either unimodal or exponential distribution of binding sites of the adsorbents studied. Though in the present study the proposed models are applied to activated carbons and for gas phase systems, it is expected that this model can be used to calculate the energy distributions of molecular imprinted polymers, biomaterials, zeolites,

etc., for different target molecules from both gas and liquid phases. The only condition to use the proposed method is that the studied adsorbent/adsorbate system should be represented by the Sips isotherm; however, as a matter of fact this isotherm is one of the most successful isotherms to represent gas and liquid phase adsorption systems. The presented site energy distribution function is very simple and is ready for predicting the site energy distributions of other systems just using the isotherm parameters that can be predicted easily by a linear or nonlinear regression analysis. The proposed model can be used to compare the performance of gas storage materials, especially the materials designed for the storage of hydrogen, natural gas, etc. Further, this method does not utilize any complex or sophisticated computer programs and can be considered as a reliable method as this method directly uses the adsorption isotherms that implicitly reflect the actual process at the studied or targeted conditions.

APPENDIX

The Sips isotherm is given by[8,9]

$$n = \frac{n_{max} K_s P^{m_s}}{1 + K_s P^{m_s}} \tag{A1}$$

The site energy distribution function according to a condensation approximation method is given by[6,10]

$$f(E^*) = -\frac{dq(E^*)}{dE^*} \tag{A2}$$

The relation between the adsorption equilibrium pressure and the saturation vapor pressure, according to the Cerofolini approximation, is given by[6,10]

$$p = p_s \exp\left(-\frac{E^*}{RT}\right) \tag{A3}$$

Then the site energy distribution function of a Sips isotherm can be obtained by substituting eq A3 in eq A1 for equilibrium pressure and then differentiating the resulting equation with respect to energy, E^*, as follows

$$f(E^*) = \frac{n_{max} K_s \left(P_s \exp\left(-\frac{E^*}{RT}\right)\right)^{m_s}}{1 + K_s \left(P_s \exp\left(-\frac{E^*}{RT}\right)\right)^{m_s}} \tag{A4}$$

For the sake of convenience, let us rename the constants and variables in eq A4 as follows: $n_{max} = A$, $K_s = B$, $P_s = P$, $E^* = x$, $RT = R$ and $m_s = m$. Thus, eq A4 can be rewritten as

$$f(x) = \frac{AB\left(P \exp\left(-\frac{x}{R}\right)\right)^m}{1 + B\left(P \exp\left(-\frac{x}{RT}\right)\right)^m} \tag{A5}$$

If $u = (P \exp(-x/R))^m$ and $v = 1 + B(P \exp(-x/RT))^m$, then using the quotient rule, $(d/dx)(u/v) = \{[(du/dx)v - u(dv/dx)]/v^2\}$, we get

$$f(x) = \frac{AB\left(\left(\left(B\left(P \exp\left(-\frac{x}{R}\right)\right)^m + 1\right)\right)\frac{d}{dx}\left(\left(P \exp\left(-\frac{x}{R}\right)\right)^m\right) - \left(P \exp\left(-\frac{x}{R}\right)\right)^m \left(\frac{d}{dx}\left(B\left(P \exp\left(-\frac{x}{R}\right)\right)^m + 1\right)\right)\right)}{\left(B\left(P \exp\left(-\frac{x}{R}\right)\right)^m + 1\right)^2} \tag{A6}$$

If $u = P \exp(-x/R)$ and $n = m$, then applying the chain rule $(du^n/dx) = nu^{n-1}(du/dx)$ and simplifying the resulting expression, we get

$$= \frac{AB\left(m\left(P \exp\left(-\frac{x}{R}\right)\right)^{m-1}\left(B\left(P \exp\left(-\frac{x}{R}\right)\right)^m + 1\right)\frac{d}{dx}\left(\exp\left(-\frac{x}{R}\right)\right) - \left(P \exp\left(-\frac{x}{R}\right)\right)^m \left(B\frac{d}{dx}\left(\left(P \exp\left(-\frac{x}{R}\right)\right)^m\right)\right)\right)}{\left(B\left(P \exp\left(-\frac{x}{R}\right)\right)^m + 1\right)^2} \tag{A7}$$

If $u = -x/R$, then by applying the chain rule, $(de^u/dx) = e^u(du/dx)$, we get

$$f(x) = \frac{AB\left(mP \exp\left(-\frac{x}{R}\right)\left(P \exp\left(-\frac{x}{R}\right)\right)^{m-1}\left(B\left(P \exp\left(-\frac{x}{R}\right)\right)^m + 1\right)\frac{d}{dx}\left(-\frac{x}{R}\right) - B\left(P \exp\left(-\frac{x}{R}\right)\right)^m \frac{d}{dx}\left(\left(P \exp\left(-\frac{x}{R}\right)\right)^m\right)\right)}{\left(B\left(P \exp\left(-\frac{x}{R}\right)\right)^m + 1\right)^2} \tag{A8}$$

dx.doi.org/10.1021/je101240f |J. Chem. Eng. Data 2011, 56, 2218–2224

Since $d(x^n) = nx^{n-1}$, eq A8 can be further simplified to

$$f(x) = \frac{AB\left(-B\left(P\exp\left(-\frac{x}{R}\right)\right)^m \frac{d}{dx}\left(\left(P\exp\left(-\frac{x}{R}\right)\right)^m\right) - \frac{mP\exp\left(-\frac{x}{R}\right)\left(P\exp\left(-\frac{x}{R}\right)\right)^{m-1}\left(B\left(P\exp\left(-\frac{x}{R}\right)\right)^m + 1\right)}{R}\right)}{\left(B\left(P\exp\left(-\frac{x}{R}\right)\right)^m + 1\right)^2} \tag{A9}$$

If $u = P\exp(-x/R)$ and $n = m$, then again using the chain rule, $(du^n/dx) = nu^{n-1}(du/dx)$, we get

$$f(x) = \frac{AB\left(\frac{-BmP\left(P\exp\left(-\frac{x}{R}\right)^{2m-1}\frac{d}{dx}\left(\exp\left(-\frac{x}{R}\right)\right)\right)}{R} - \frac{mP\exp\left(-\frac{x}{R}\right)\left(P\exp\left(-\frac{x}{R}\right)\right)^{m-1}\left(B\left(P\exp\left(-\frac{x}{R}\right)\right)^m + 1\right)}{R}\right)}{\left(B\left(P\exp\left(-\frac{x}{R}\right)\right)^m + 1\right)^2} \tag{A10}$$

Again, if $u = -x/R$, then by applying the chain rule $(de^u/dx) = e^u(du/dx)$, we get

$$f(x) = \frac{AB\left(-BmP\exp\left(-\frac{x}{R}\right)\left(P\exp\left(-\frac{x}{R}\right)^{2m-1}\frac{d}{dx}\left(-\frac{x}{R}\right)\right) - \frac{mP\exp\left(-\frac{x}{R}\right)\left(P\exp\left(-\frac{x}{R}\right)\right)^{m-1}\left(B\left(P\exp\left(-\frac{x}{R}\right)\right)^m + 1\right)}{R}\right)}{\left(B\left(P\exp\left(-\frac{x}{R}\right)\right)^m + 1\right)^2} \tag{A11}$$

Again, if $u = -x/R$, then by applying the chain rule $(de^u/dx) = e^u(du/dx)$, we get

$$f(x) = \frac{AB\left(\frac{BmP\left(-\frac{x}{R}\right)\left(P\exp\left(-\frac{x}{R}\right)^{2m-1}\frac{d}{dx}(x)\right)}{R} - \frac{mP\exp\left(-\frac{x}{R}\right)\left(P\exp\left(-\frac{x}{R}\right)\right)^{m-1}\left(B\left(P\exp\left(-\frac{x}{R}\right)\right)^m + 1\right)}{R}\right)}{\left(B\left(P\exp\left(-\frac{x}{R}\right)\right)^m + 1\right)^2} \tag{A12}$$

Since we know that $d(x^n) = nx^{n-1}$, eq A12can be further simplified to

$$f(x) = \frac{AB\left(\frac{BmP\left(-\frac{x}{R}\right)\left(P\exp\left(-\frac{x}{R}\right)^{2m-1}\right)}{R} - \frac{mP\exp\left(-\frac{x}{R}\right)\left(P\exp\left(-\frac{x}{R}\right)\right)^{m-1}\left(B\left(P\exp\left(-\frac{x}{R}\right)\right)^m + 1\right)}{R}\right)}{\left(B\left(P\exp\left(-\frac{x}{R}\right)\right)^m + 1\right)^2} \tag{A13}$$

dx.doi.org/10.1021/je101240f |J. Chem. Eng. Data 2011, 56, 2218–2224

Expanding the above expression and adding or canceling the similar terms, the above equation can be simplified to

$$f(x) = \frac{ABm\left(P\exp\left(-\frac{x}{R}\right)\right)}{\left(B\left(P\exp\left(-\frac{x}{R}\right)\right)^{m}+1\right)^{2}R} \quad \text{(A14)}$$

Replacing the constants or variables by their original notations, $A = n_m$, $B = K_s$, $P = P_s$, $x = E^*$, $R = RT$, and $m = m_s$, we get

$$f(E^*) = \frac{n_{max}k_s m_s p_s\left(\exp\left(-\frac{E^*}{RT}\right)\right)^{m_s}}{\left(k_s\left(p_s\exp\left(-\frac{E^*}{RT}\right)\right)^{m_s}+1\right)^{2}RT} \quad \text{(A15)}$$

AUTHOR INFORMATION

Corresponding Author

*E-mail: vasanth@ua.es (K.V. Kumar); vinodfcy@ittr.ernet.in (V.K. Gupta).

Funding Sources

K.V.K. would like to thank Ministerio de Ciencia e Innovacion (Spain) for the Juan de la Cierva contract. A.S.A. acknowledges a Ph.D. fellowship from MEC, Spain.

REFERENCES

(1) Umpleby, R. J.; Baxter, S. C.; Rampey, A. M.; Rushton, G. T.; Chen, Y.; Shimizu, K. D. Characterization of the heterogeneous binding site affinity distributions in molecularly imprinted polymers. *J. Chromatogr., B* **2004**, *804*, 141–149.

(2) Umpleby, R. J.; Bode, M.; Shimizu, K. D. Measurment of the continous distribution of binding sites in molecularly imprinted polymers. *Analyst* **2000**, *125*, 1261–1265.

(3) Umpleby, R. J.; Baxter, S. C.; Chen, Y.; Shah, R. N.; Shimizu, K. D. Characterization of molecularly imprinted polymers with the Langmuir-Freundlich isotherm. *Anal. Chem.* **2001**, *73*, 4584–4591.

(4) Jaroniec, M.; Madey, R. *Physical adsorption on heterogeneous solid surfaces*; Academic Press: London, 1991.

(5) Rudzinski, W.; Everett, D. H. *Adsorption of Gases on Heterogeneous Surfaces*; Academic Press: New York, 1992.

(6) Cerofolini, G. F. Localized adsorption on heterogeneous surfaces. *Thin Solid Films* **1974**, *23*, 129–152.

(7) Silvestre-Albero, A.; Silvestre-Albero, J.; Sepúlveda-Escribano, A.; Rodríguez-Reinoso, F. Ethanol removal using activated carbon: Effect of porous structure and surface chemistry. *Microporous Mesoporous Mater.* **2009**, *120*, 62–68.

(8) Sips, R. On the structure of a catalyst surface. *J. Chem. Phys.* **1948**, *16* (5), 490–495.

(9) Sips, R. On the structure of a catalyst surface, II. *J. Chem. Phys.* **1950**, *18* (8), 1024–1026.

(10) Carter, M. C.; Kilduff, J. E.; Weber, W. J., Jr. Site Energy Distribution Analysis of Preloaded Adsorbents. *Environ. Sci. Technol.* **1995**, *29*, 1773–1780.

(11) Park, J.-W.; Lee, S.-S.; Choi, D.-K.; Lee, Y.-W.; Kim, Y.-M. Adsorption equilibria of toluene, dichloromethane, and trichloroethylene onto activated carbon fiber. *J. Chem. Eng. Data* **2002**, *47* (4), 980–983.

(12) Guan, C.; Loo, L. S.; Yang, C.; Wang, K. Sorption properties of a single wall carbon nanotube. *J. Chem. Eng. Data* **2008**, *53* (10), 2451–2453.

(13) Ali, I.; Gupta, V. K. Advances in water treatment by adsorption technology. *Nat. Protoc.* **2007**, *1*, 2661–2667.

(14) Gupta, V. K.; Ali, I. Removal of Endosulfan and Methoxychlor from Water on Carbon Slurry. *Environ. Sci. Technol.* **2008**, *42*, 766–770.

(15) Gupta, V. K.; Mittal, A.; Kurup, L.; Mittal, J. Adsorption of basic fuchsin using waste materials - bottom ash and de-oiled soya as adsorbents. *J. Colloid Interface Sci.* **2008**, *319*, 30–39.

(16) Gupta, V. K.; Carrott, P. J. M.; Ribeiro Carrott, M. M. L.; Suhas. Low cost adsorbents: Growing approach to wastewater treatment - A review. *Crit. Rev. Environ. Sci. Technol.* **2009**, *39*, 783–842.

(17) Gupta, V. K.; Suhas. Application of low cost adsorbents for dye removal- A review. *J. Environ. Manage.* **2009**, *90*, 2313–2342.

(18) Gupta, V. K.; Ali, I.; Saini, V. K. Adsorption studies on the removal of Vertigo Blue49 and Orange DNA13 from aqueous solutions using carbon slurry developed from a waste material. *J. Colloid Interface Sci.* **2007**, *315*, 87–93.

(19) Gupta, V. K.; Jain, R.; Varshney, S. Removal of Reactofix golden yellow 3 RFN from aqueous solution using wheat husk- an agricultural waste. *J. Hazard. Mater.* **2007**, *142*, 443–448.

(20) Gupta, V. K.; Mittal, A.; Jain, R.; Mathur, M.; Sikarwar, S. Adsorption of Safranin-T from Wastewater Using Waste Materials - Activated Carbon and Activated Rice Husk. *J. Colloid Interface Sci.* **2006**, *303*, 80–86.